Repairability-Based Design of Concrete Structures

Eyitayo A. Opabola
Senior Research Fellow, Dept. of Civil, Environmental, and Geomatic Engineering, University College London, London, United Kingdom

Kenneth J. Elwood
Professor, Dept. of Civil and Environmental Engineering, University of Auckland, Auckland, New Zealand

ABSTRACT: The economic and environmental impacts associated with the demolition and long-term closure of damaged modern buildings in recent earthquakes (e.g., 2010/2011 Canterbury earthquakes) led to societal demands for improved design procedures to limit damage and shorten recovery time after earthquakes. To address these societal demands, this study proposes a repairability-based design approach for structural systems. The proposed approach aims to ensure that, under design-level earthquakes, damaged structural components have sufficient residual capacity to withstand future events without requiring safety-critical repair. Firstly, the repairability limit state for RC components is defined using an extensive database of past tests on RC components. Subsequently, component deformation limits are proposed for RC beams and columns. Furthermore, nonlinear response history and recovery analyses of four archetype frame buildings, designed per New Zealand standards to different beam deformation limits, are used to assess the seismic performance and capability of the buildings to satisfy recovery-based performance objectives. By comparing the repairability fragility and functional recovery downtime estimates of the frame buildings for design-level events, it is concluded that it is feasible for the building code to target repairability in the design-basis earthquake in addition to collapse prevention in the maximum considered earthquake.

1. INTRODUCTION

Recent earthquakes (e.g.,2010/2011 Canterbury earthquakes) demonstrated that modern reinforced concrete (RC) buildings will satisfy the code-intended life safety performance objectives. However, repair costs and downtime of damaged modern buildings have been considered uneconomic (Marquis et al. 2017). Furthermore, the environmental effects from pollution associated with building demolitions and (re)construction-related carbon impacts are becoming unacceptable. It has also been highlighted that a significant gap exists between codified design provisions and desired performance objectives by building owners and society at large (Brown et al. 2022; EERI 2019). Policymakers and the engineering community are beginning to advocate for improved seismic design provisions which help to reduce post-disaster functionality loss and improve recovery time (EERI 2019; FEMA 2021b; Senate Bill 1768 2018). Such provisions would target a high likelihood of functional recovery by ensuring (a) limited damage to non-structural systems and (b) that induced structural damages will not compromise the residual capacity of the buildings for future events (including aftershocks).

To address this, the current study presents a repairability-based design approach as a key step towards addressing recovery-based objectives for buildings. The design approach can be applied to all structural systems, irrespective of construction materials. Herein, the repairability limit state is defined as the post-earthquake state beyond which the strength and deformation capacity of a structural component is compromised, and its performance in a future event cannot be guaranteed without safety-critical repair.

In line with the objectives, this study focuses on developing repairability limit states for RC systems. Using an extensive database of past tests on RC components, design component deformation limits (corresponding to the repairability limit state) are defined for RC beams and columns. Thereafter, nonlinear response history and recovery (using the ATC-138 methodology) analyses of four archetype frame buildings, designed per New Zealand standards to different beam deformation limits, are used to assess the seismic performance and capability of the buildings to satisfy recovery-based performance objectives.

2. ADDRESSING RECOVERY-BASED OBJECTIVES BY DESIGNING FOR REPAIRABILITY

Performance-based seismic design (PBSD) allows for the selection of appropriate ground motion levels and corresponding performance objectives for the structural and non-structural components in a building. The performance objective could range from full functionality to collapse prevention. According to FEMA P-2090 (FEMA 2021b), re-occupancy and functional recovery objectives are collectively referred to as recovery-based objectives. Re-occupancy has been defined as the post-disaster performance state whereby the building is maintained/restored to be safe enough to serve as shelter, even if critical utility systems are not in functioning states (FEMA 2021b). Functional recovery is a post-disaster performance state in which a structural system is maintained/restored to safely and adequately support its pre-earthquake intended functions (FEMA 2021b).

Figure 1 is a conceptual representation of a PBSD framework including recovery-based objectives. As shown in the Figure, the structural design is governed by the repairability assessment aimed at evaluating if the repairability limit state is exceeded at the desired intensity level. Essentially, a building with components that have exceeded the repairability limit state would be unlikely to satisfy recovery-based objectives and likely unoccupiable following a design-level event.

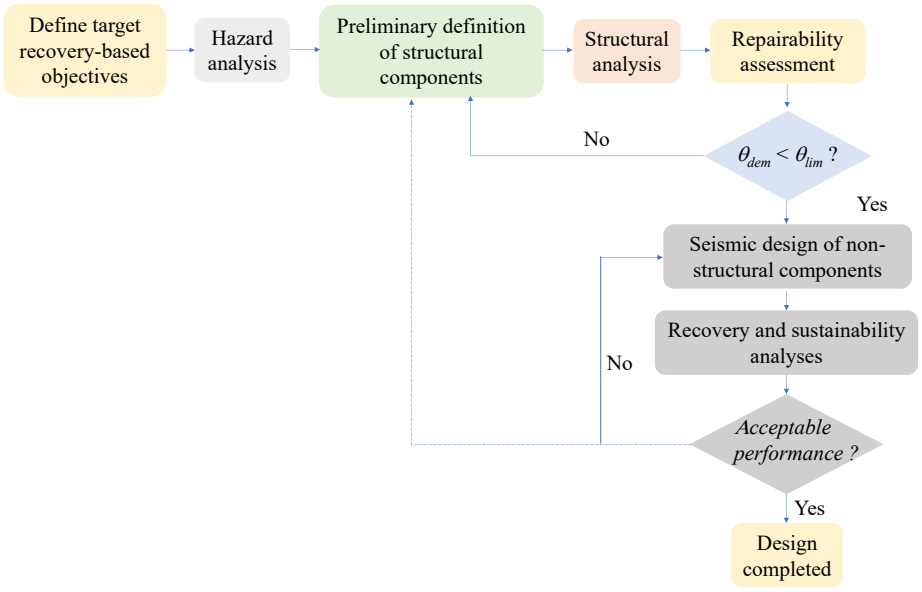

Figure 1 – Repairability-based requirement within a conceptual recovery-targeted performance-based seismic design framework

As shown in Figure 1, the structural system is iteratively designed until all structural components are repairable at the target hazard level. Of course, to holistically achieve recovery-

based objectives, non-structural components must also satisfy the intended performance objective at this target hazard level (See Figure 1). Once the structural systems are designed to be 'repairable', appropriate non-structural systems are selected and designed to accommodate the design deformation/floor acceleration demands. Detailed discussions on the design of non-structural elements are outside the scope of this paper.

Following the design of structural and non-structural component systems, recovery analyses can be carried out to assess the range of expected downtime for the designed building at various intensity levels. A number of studies (e.g., Almufti and Willford (2013) and Cook et al. (2022)) have proposed recovery analysis frameworks. Engineers can use any recovery analysis frameworks they prefer, provided it accounts for the expected post-disaster recovery impeding factors. The current study uses the ATC-138 framework (FEMA 2021a) to demonstrate that a building satisfying proposed repairability limits for the DBE will have a high probability of also meeting key recovery targets.

3. COMPONENT DEFORMATION LIMITS FOR REPAIRABILITY REQUIREMENTS

In a separate study aimed at developing guidance for post-earthquake assessment and repair of earthquake-damaged structures, Opabola et al. (2023) examined datasets of ductile RC beam, column, and wall specimens subjected to various loading protocols. The main objectives of the study were to understand (a) the deformation demand beyond which the residual capacity of the RC component is compromised; and (b) the influence of prior loading history on future performance. The authors concluded that provided that the deformation at the initiation of lateral strength loss (LSL) of an RC component is not exceeded in any previous loading histories and low-cycle fatigue is not triggered, aside from a reduction in initial stiffness, the residual capacity (in terms of strength and deformation capacity) of the component is unlikely to be compromised. The authors compared the deformation at the initiation of lateral strength loss for a database of ductile beam, column, and wall specimens and concluded that the deformation at the initiation of lateral strength loss typically corresponds to the onset of bar buckling in the test specimens (with a coefficient of variation less than 20%).

To avoid observational uncertainty associated with the reported drifts at the onset of bar buckling in tests, Opabola et al. (2023) adopt the drift at LSL as the deformation limit corresponding to the repairability limit state. For consistency purposes, the current study follows the Opabola et al. (2023) approach. Figure 2 presents the measured drift at LSL for the ductile specimens in the Opabola et al. (2023) database. It can be inferred from Figure 2a, that the drift at LSL for well-confined beams is independent of the ratio of stirrup spacing to bar diameter (s/d_b).

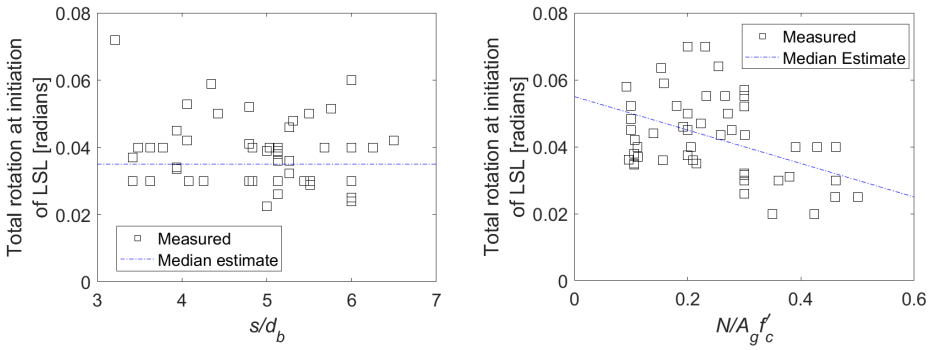

(a) Beams (b) Columns

Figure 2 – Measured deformation at LSL for (a) ductile beams (b) ductile columns (See Opabola et al. 2023 for details on the data)

The lognormal CDF fitted to the beam dataset corresponds to a median deformation at LSL of 3.6% with a logarithmic dispersion of 0.25. As shown in Figure 2b, the drift at LSL for columns is dependent on the axial load ratio. Relationships for the median estimates for drift at LSL as a function of axial load ratio $(N/A_g f'_c)$ are shown in Figure 2b.

Equation (1) provide median estimates for the total chord rotation at LSL for ductile columns with a logarithmic dispersion of 0.26 for the columns datasets.

$$\theta_{c,LSL} = 0.056 - 0.06\frac{N}{A_g f'_c} \leq 0.05 \qquad (1)$$

From a probabilistic assessment point of view, for a structure to be repairable, there has to a low likelihood of the deformation demands from a given hazard level exceeding the deformation at LSL, accounting for all sources of epistemic and aleatory uncertainties. Considered uncertainties include: (a) uncertainty in predicting the deformation at LSL β_{LSL} (estimated as 0.3 for both beams and columns) , (b) uncertainty in the influence of loading history on the drift capacity at LSL β_{LP} (estimated as 0.16 from test data), (c) design requirements uncertainty (β_{DR}) (taken as 0.2 (FEMA 2009)) (d) construction quality assurance β_{CQ} (taken as 0.1 (FEMA 2012)), (e) Modeling uncertainty β_M (taken as 0.25 (FEMA 2012)), and (f) record-to-record uncertainty β_{RTR} (taken as 0.4 (FEMA 2012)).

The uncertainty sources are combined through square root of sum of squares to give a combined uncertainty β_{TOT} of about 0.65. Based on this β_{TOT}, selected probabilities of 0.05, 0.1, 0.15 and 0.2 result in repairability margin ratios of 0.34, 0.46, 0.51, and 0.58. For beams with a median drift at LSL of 3.6%, a design component deformation limit of 0.58*3.6 = 2% can be estimated for a selected probability of 0.2. Also, component deformation limits of about 1% and 1.5% correspond to probabilities of exceedance of 0.05 and 0.1, respectively.

4. NUMERICAL ANALYSES OF MODERN-CODE AND REPAIRABLE BUILDINGS

4.1. Overview

This section explores the seismic performance and likelihood of modern-code buildings and buildings meeting a repairability limit state to satisfy recovery-based performance objectives. Firstly, four archetype buildings are designed to different beam rotation limits – 1.5%, 2%, 2.5%, and 3%, corresponding to 0.1, 0.2, 0.3, and 0.4 probabilities of exceeding the beam repair limit. As earlier mentioned, beam rotation limits will govern a frame building design, except when the columns are under high axial load. The four buildings are named based on the design beam rotation (BR) as BR_1.5, BR_2, BR_2.5, and BR_3, respectively. Following the archetype designs, nonlinear response history analyses (NLRHA) are carried out to derive and compare fragilities for safety-critical repair (i.e., repairability) and collapse limit states for the four buildings. Interstory drift and peak floor acceleration outputs from the NLRHA are used to conduct recovery analyses of the archetypes using the ATC-138 methodology (FEMA 2021a). A description of the ATC 138 methodology is provided subsequently in this paper. Finally, the fragilities and recovery times for the four buildings are compared.

4.2. Archetype design

The archetype buildings are five-story regular RC perimeter frame buildings located on a Site Class C in Wellington. The plan and elevation views of the building are presented in Figure 3. The buildings are designed per NZS 1170.1, NZS 1170.5, and NZS 3101 (Standards New Zealand 2002, 2004, 2006).

The four target design beam rotations (i.e., 1.5%, 2%, 2.5%, and 3%) was achieved by varying the dimensions of the beams and columns in each archetype. The design interstory drift demands were scaled from the elastic drift demands following NZS 1170.5 provisions. Design beam rotation (θ_b) was computed from the

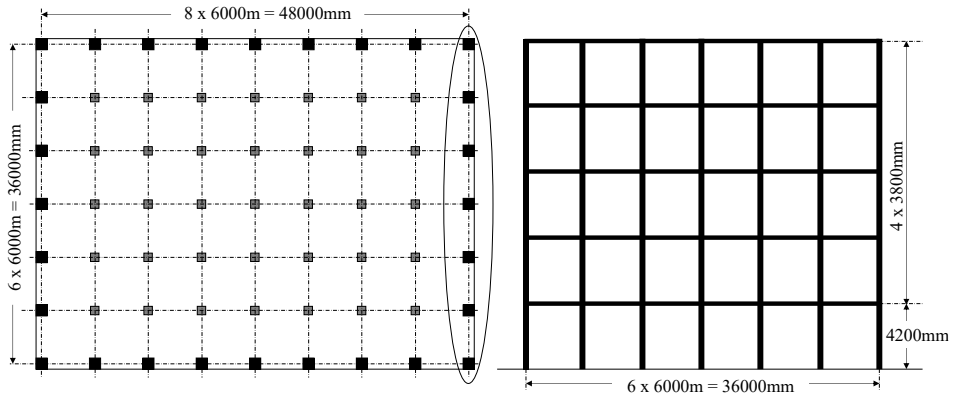

(a) Plan view (b) Elevation

Figure 3 – Plan and elevation views of the archetypes (the modelled seismic frame is circled in (a))

interstory drift ratio (θ_c) according to CCANZ (2011).

4.3. Numerical modelling

Two-dimensional nonlinear finite element models of the 36m long seismic frame were developed in OpenSees using concentrated plasticity models. The OpenSees Modified IMK hinge was adopted in this study. To properly simulate the response of the beams, the moment-rotation behavior of the beams was calibrated to the force-displacement responses of beams tested at the University of Auckland Structures Laboratory (Marder et al. 2018). The moment-rotation behavior of the columns were modelled following the recommendations of Haselton et al. (2016). To account for joint flexibility, in accordance to ASCE/SEI 41 (ASCE 2017), rigid offsets were only assumed in the columns. To account for nonlinear geometric effects in the OpenSees model, P-delta transformation was adopted for the seismic columns. Furthermore, a leaning column (with a pinned base) connected to the seismic frame via a rigid truss element was used to simulate the gravity load on the interior gravity columns of the structure. A 2% Rayleigh damping in the first and third modes was adopted for the model. The natural periods for the buildings are 1.0s, 1.2s, 1.45s, and 1.7s, respectively.

The corresponding elastic response spectrum for the site conditions of the building, defined using NZS 1170.5, was used to select ground motions at five intensity levels – return period of 50, 100, 500, 1000, and 2500 years. The ground motion selection and scaling procedure at each intensity level were in accordance with NZS 1170.5. A total of 11 ground motion records were selected at each intensity level.

4.4. Seismic fragility at repairability and collapse limit states

By assuming a lognormal distribution for the demand and capacity, the probability of exceeding a specified limit state in the structural components can be estimated using Equation (2):

$$P\left[D > C \middle| \mathrm{IM}\right] = \Phi\left[\frac{\ln\left(S_D/S_C\right)}{\sqrt{\beta_{D|\mathrm{IM}}^2 + \beta_C^2 + \beta_{LP}^2 + \beta_{DR}^2 + \beta_{CQ}^2 + \beta_M^2}}\right] \quad (2)$$

where D is the seismic demand, C is the structural capacity, S_D is the median value of the demand, S_C is the median value of the structural limit state, $\beta_{D|IM}$ is the record-to-record variability as a function of $S_a(T_1)$, β_C is the dispersion of drift capacity at the considered limit state, β_{DR} is the design requirements uncertainty, β_{CQ} is the construction quality assurance, and β_M is the modeling uncertainty.

The median component capacity at the repairability limit state is based on the definition provided in the earlier sections. Collapse was defined to correspond to an interstory drift ratio of 6%.

Figure 4 presents the resulting fragility curves for the considered buildings. Figure 4d shows that the 'code-minimum' building (i.e., BR_3) has a median safety-critical repair fragility

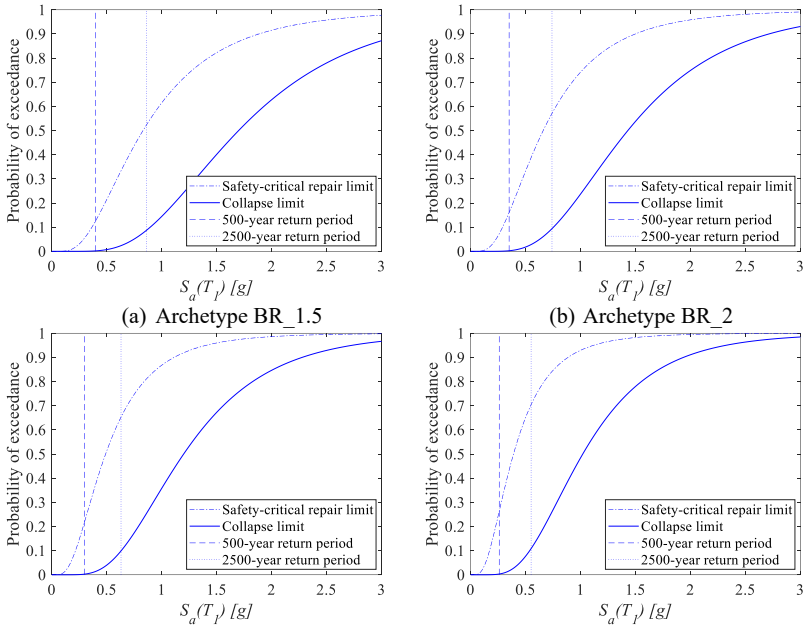

(a) Archetype BR_1.5 (b) Archetype BR_2

(c) Archetype BR_2.5 (d) Archetype BR_3

Figure 4 – Seismic fragility curves for safety-critical repair and collapse limit states for the four archetypes

of 0.4g, while the buildings designed to beam rotation limits of 2% and 1.5% have median safety-critical repair fragilities of 0.66g and 0.83g, respectively – corresponding to a 65% and 100% increase, respectively.

4.5. Recovery analyses

The ATC-138 recovery analysis methodology (FEMA 2021a) was adopted in this study. The methodology uses structural analysis outputs (i.e., peak interstory drift ratio and floor accelerations) to quantify the post-earthquake recovery state of a building at the component- and system-levels in a probabilistic manner. The main outputs of the methodology are probabilistic distributions for the times required to achieve re-occupancy, functional recovery, and full recovery.

The ATC-138 methodology quantifies the probabilistic post-earthquake recovery state of a building by estimating the post-earthquake damage states of the structural and non-structural components in the building and evaluating system-level performance through a series of fault-tree analyses. The time required to restore a building to a particular recovery state uses a repair scheduling algorithm which accounts for recovery-impeding factors associated with the inspection of a damaged building, design and permitting, contractor mobilization, temporary clean-up and repairs, and other factors. It is noted that the framework assumes that financing, engineering design, permit procurement, and contractor mobilization take place in parallel. Also, the estimated times depend on the severity of the damage to the building. There is significant uncertainty in estimating these time frames, hence the distribution of potential time frames is an important output of the methodology. Further discussions on the ATC-138 methodology can be found in FEMA (2021) and Cook et al. (2022).

Figure 5 presents the outputs of the recovery analyses (i.e., estimated functional recovery times) for the four archetypes at five intensity levels. As shown in Figure 5, the downtime to achieve functional recovery for the four archetypes varies significantly at design-level (i.e.

500 years), with buildings designed to repairability-based limits exhibiting a higher probability of achieving immediate functional recovery in comparison to code-minimum buildings for design-level events. A median downtime of about six months is required to achieve functional recovery in the code-minimum building at design-level. On the other hand, the median results indicate that the repairable buildings (i.e., BR_1.5 and BR_2) are able to achieve immediate functional recovery at design-level demands. Considering the median results, archetype BR_1.5 achieves immediate functional recovery for ground motion intensities up to 1000-year return period, while archetype BR_2 is able to achieve a similar performance up to 500 year return period.

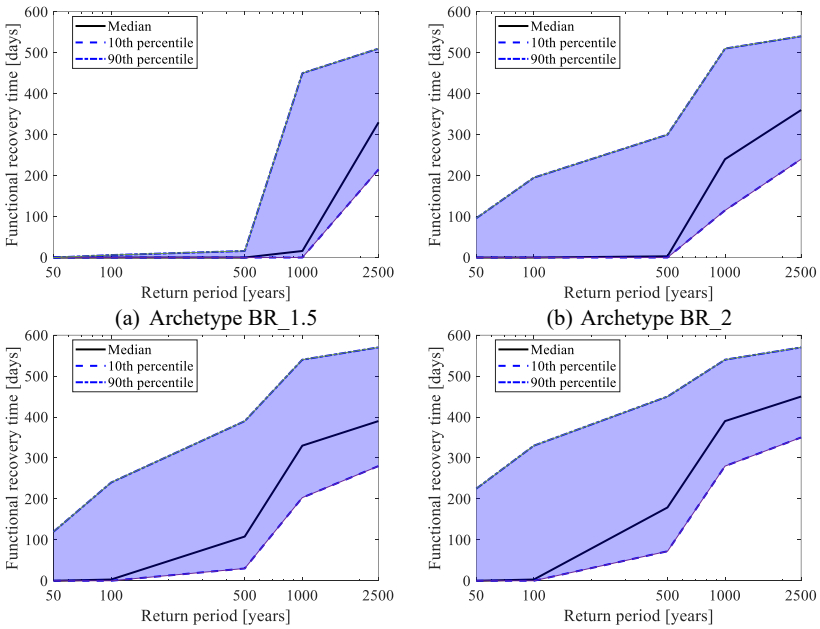

(a) Archetype BR_1.5 (b) Archetype BR_2

(c) Archetype BR_2.5 (d) Archetype BR_3

Figure 5 – Estimated functional recovery time for the four archetypes using the ATC-138 methodology

5. DISCUSSIONS AND CONCLUSIONS

Figure 6 compares the influence of the design beam rotation on the median time to achieve functional recovery for 500-year return period ground motions. The Figure also includes for the four archetypes the probability of exceeding the safety-repair limit state (RLS) and collapse limit state (CLS) for 500-year and 2500-year return period ground motions, respectively. Note that all buildings have a probability of requiring safety-critical repairs of less than 50%, even for the code-minimum design (BR_3) where the component limits were not considered in the design process. This suggests that modern code-designed buildings are likely to be repairable in a design-level earthquake. However, the median functional recovery time frame for the code-minimum building of approximately 6 months may be considered too long. Designing to satisfy the repair component limits suggested in this study (BR_2) leads to a median functional recovery time on the order of days, a 40 times reduction relative to the code-minimum building. As earlier mentioned, Figure 6 suggests that the probability of exceeding the repairability limit state in DBE is more affected by the change in design hinge rotations than the collapse probability in MCE (i.e, increased stiffness affects reparability more than collapse performance).

For codification purposes, it is important for decision-makers to identify the appropriate target hazard level for defining repairable buildings. Hence, it is recommended that hazard curves be combined with safety-critical repair fragility

functions to assess the risk of requiring safety-critical repairs during the design service life. Further studies, considering a range of hazard curves, need to carried out to develop a uniform-risk-targeted repairability-based seismic design approach.

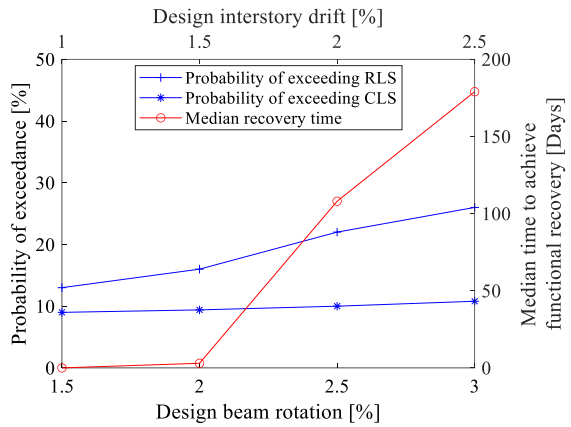

Figure 6 – Relationship between the design deformation limits, median functiona recovery time under a 500-year return period, and probability of exceeding the safety-repair limit state (RLS) under a 500-year return period and collapse limit state (CLS) under a 2500-year return period for the four archetypes

6. REFERENCES

Almufti, I., and Willford, M. (2013). "The resilience-based earthquake design initiative (REDi^{TM}) rating system." (October), 1–133.

ASCE. (2017). *Seismic Evaluation and Retrofit of Existing Buildings: ASCE/SEI 41-17*. American Society of Civil Engineers, Reston, VA.

Brown, C., Abeling, S., Horsfall, S., Ferner, H., and Cowan, H. (2022). *Societal Expectations for Seismic Performance of Buildings*. Wellington, NZ.

CCANZ. (2011). *Examplesof concrete structural design to New Zealand Standard 3101*. Cement & Concrete Association of New Zealand.

Cook, D. T., Liel, A. B., Haselton, C. B., and Koliou, M. (2022). "A framework for operationalizing the assessment of post-earthquake functional recovery of buildings." *Earthquake Spectra*, SAGE Publications Sage UK: London, England, 87552930221081540.

EERI. (2019). *Functional recovery: A conceptual framework with policy options*.

FEMA. (2009). *Quantification of building seismic performance factors, FEMA P-695. FEMA P695*, prepared by Applied Technology Council for the Federal Emergency Management Agency, Washington, D.C.

FEMA. (2012). *Seismic performance assessment of buildings: FEMA P58 guidelines*. Redwood City, California.

FEMA. (2021a). *ATC-138-3: Seismic Performance Assessment of Buildings Volume 8 – Methodology for Assessment of Functional Recovery Time*.

FEMA. (2021b). *FEMA P-2090/NIST SP-1254: Recommended Options for Improving the Built Environment for Post-Earthquake Reoccupancy and Functional Recovery Time*. Gaithersburg, MD.

Haselton, C. B., Liel, A. B., Taylor-Lange, S. C., and Deierlein, G. G. (2016). "Calibration of model to simulate response of reinforced concrete beam-columns to collapse." *ACI Structural Journal*, 113(6), 1141–1152.

Marder, K., Motter, C., Elwood, K. J., and Clifton, G. C. (2018). "Testing of 17 identical ductile reinforced concrete beams with various loading protocols and boundary conditions." *Earthquake Spectra*, SAGE Publications Sage UK: London, England, 34(3), 1025–1049.

Marquis, F., Kim, J. J., Elwood, K. J., and Chang, S. E. (2017). "Understanding post-earthquake decisions on multi-storey concrete buildings in Christchurch , New Zealand." *Bulletin of Earthquake Engineering*, 15, 731–758.

Opabola, E. A., Abdullah, S. A., Elwood, K. J., and Wallace, J. W. (2023). "Limit States for Post-Earthquake Assessment and Recovery Analysis of Ductile Concrete Components." *Earthquake Spectra*, (Accepted)

Senate Bill 1768. (2018). *National Earthquake Hazards Reduction Program Reauthorization Act of 2018*.

Standards New Zealand. (2002). *NZS 1170.1:2002 Structural design actions. Part 1: Permanent, imposed and other actions*.

Standards New Zealand. (2004). *NZS 1170.5 Supp 1:2004 - Structural Design Actions – Part 5 Earthquake Actions – New Zealand*. Wellington, NZ.

Standards New Zealand. (2006). *NZS 3101:2006:A3 - Concrete structures standard.* Wellington, NZ.